On the structure and mechanical behaviour of the extending lithosphere in the Baikal Rift from gravity modelling

Carole Petit [a,*], Evgene Burov [b,1], Jacques Déverchère [a]

[a] *Laboratoire de Géodynamique sous-marine, UMR Géosciences Azur, La Darse, BP 48, 06230 Villefranche-sur-mer, France*
[b] *Laboratoire de Gravimétrie et Géodynamique, Institut de Physique du Globe, 4 place Jussieu, 75005 Paris, France*

Abstract

The crustal structure and lithospheric flexure of the Baikal Rift Zone, Siberia, are examined by means of gravity modelling. We model the Bouguer Anomaly (BA) along five 1200 km long gravity profiles. We first evidence that continuous elastic plate flexure due to surface loading cannot explain the observed BA. Then we introduce plate discontinuities coupled with a realistic brittle–elasto-ductile plate rheology, which allow us to model of external tectonic forces acting on the plates and determination of the Moho geometry. We show that the clearest expression of extensional processes occurs in the central part of the rift, which exhibits the highest crustal thinning. It evolves southwards to a rapidly increasing compression, resulting in an overthickening of the southern plate's crust and in the long-wavelength flexure of the Siberian plate. North of the central rift, crustal thinning (which is always less than 7 km) gives way to a more diffuse zone of deformation inside the Sayan–Baikal folded belt. Based on plate flexure models, we propose that the rift shoulders surrounding the central and north Baikal basins are not supported by upward bending plate, but have a deep crustal root caused by a downward flexure. The other parts of the rift depict two adjacent plates with antithetic flexures. We also infer that the axial mantle material upwarping is not related to a large-scale asthenospheric upwelling, since the lithosphere rheological interfaces are not significantly disturbed.

Our results favour the role of horizontal forces and motions, resulting from the India–Asia collision, combined with the effect of inherited tectonic structures (and especially the Paleozoic suture bounding the Siberian craton) for explaining the crustal structure and plate flexure modeled.

Keywords: rifting; gravity surveys; models; crustal thinning; Baikal rift zone

1. Introduction

The existence and development of intracontinental rifts are governed by extensional stresses originated either at far-field plate boundaries or at nearby deep lithospheric levels, acting on a complex, heterogeneous lithosphere [1]. Lithospheric extension generates thermal disturbances and isostatic reactions expressed by vertical movements such as basin subsidence and rift flank uplift [2–5]. The mechanical response of the lithosphere to extensional processes is controlled by various factors like the rheology, the pre-rift lithospheric structure, and the strain rate,

* Corresponding author. Fax: +33 4 9376 3746. E-mail: petit@ccrv.obs-vlfr.fr
[1] Now at: Bureau des Recherches Géologiques et Minières, Direction de la Recherche, Av. C. Guillemin, BP 6009, 45060 Orléans Cedex 2, France.

which determine the rift morphology and the style of the extensional deformation (e.g., [6–8]).

Despite the variability of these parameters, many present-day rift systems generally share some major characteristics. For example, variable amounts of crustal and lithospheric thinning have been imaged by gravity and seismic studies in the Rio Grande [9,10], East African [11–13] and Rhine Graben [14] rifts. Associated upwarping of anomalous mantle and high heat flow values are reported by several authors (around 100–115 mW/m^2 in the Rio Grande, Rhine and Kenya rifts, see e.g., [15–18]). These observations, as well as the important amount of upper crustal brittle failure, primarily lead to the assumption that the lithosphere is subsequently weakened at the vicinity of the rift axis and hence exhibits a low mechanical strength.

However, as shown by gravity and topography modelling, the formation of long-lived high rift flanks imply that the lithosphere must retain strength during extension (e.g., [3,5,7]). The integrated lithospheric strength is usually described by the parameter EET, which is the effective elastic thickness. It ranges between 17 and 38 km in the western branch of the East African Rift [19,20] and between 15 and 30 km in the Rio Grande rift [10]. Moreover, although the seismicity is generally located within the shallow range of 20 km depth, earthquakes can occur at depths up to 25–30 km below the borders of the East African Rift [19], suggesting that the brittle–ductile transition remains deep besides the rift axis.

Compared to 'classical' examples previously mentioned, the Baikal Rift Zone (BRZ), Siberia, depicts unusual features. The average heat flow is rather low and ranges between 40 and 75 mW/m^2 [21]. Focal depths of earthquakes reach lower crust to upper mantle levels in the Northern Baikal Rift (NBR) [22], where the crust is about 42–50 km thick and exhibits no significant thinning [23,24]. Studies based on deep seismic soundings and gravity modelling in terms of local (Airy) compensation could advocate a decrease in the crustal thickness from 40–45 km in the surrounding area to 35 km beneath the rift axis, in its central part [25,26]. However, recent 1D gravity modelling tends to invalidate the hypothesis of local isostasy, and demonstrate that the lithosphere beneath the BRZ exhibits a high EET of 30–50 km [27,23,28]. The Baikal rift lithosphere

thus appears stronger and colder than other continental rift zones. However, the important variations, in nature and orientation, of the main structural features along the rift do not allow generalization of these results for the entire rift. Imaging the deep structures and the mechanical behaviour of the lithosphere in the BRZ now requires studying and correlating several gravity profiles sampling different parts of the whole rift zone. In this paper we analyze the short wavelength gravity field along 5 profiles crossing the BRZ. The use of density contrast linked to the Moho discontinuity allows us to assess the crustal structure and quantify the amount of crustal thinning. The flexural response of the lithosphere is modeled assuming realistic brittle–elasto-ductile rheology and additional horizontal and vertical boundary forces. Finally, the results are grouped and compared to previous gravity and seismic studies, in order to provide a tectonic interpretation of the inferred crustal structure and lithospheric flexure of the BRZ.

2. Data processing and gravity modelling

2.1. Data set and methodology

The gravity data used for this study are prepared on the basis of 5' × 7.5' maps (Fig. 1), previously published with the consent of the International Scientific Environmental Centre of the Russian Academy of Sciences (ISEC) [29,23]. A more detailed description of the source data can be found in [23]. Elevation data are taken from the 5' × 5' digital topography issued on CD-ROM by GETECH, which is based on an original high quality Russian military data set. Five 1200 km long representative profiles have been prepared on the basis of these data. Of these, 3 profiles (A, B and C) strike N–S and cross the Southern Baikal Rift (SBR) at the place where the main structural features (Sayan, Tunka and south Baikal faults, Tunka and south Baikal basins) strike approximately E–W or NE–SW (Fig. 2). This relatively dense sampling was felt necessary because this region, located around the southwards pointing edge of the Siberian craton (Fig. 2), shows dramatic changes in the tectonic regime, from compression in

the west to extension in the east [30], which probably affect the crustal structure and lithospheric strength.

Two other profiles (D and E) run NW–SE and NNW–SSE across the central and northern Baikal basins, respectively (Fig. 2). They allow us to study two morphologically different rift areas: profile D crosses a single, narrow basin (the central Baikal basin) which is the oldest rift depression [31], while profile E crosses a younger, wide rift zone made of two large parallel basins (north Baikal and Barguzin) [32]. Finally, in order to have a complete overview of the BRZ, we compare our results with those
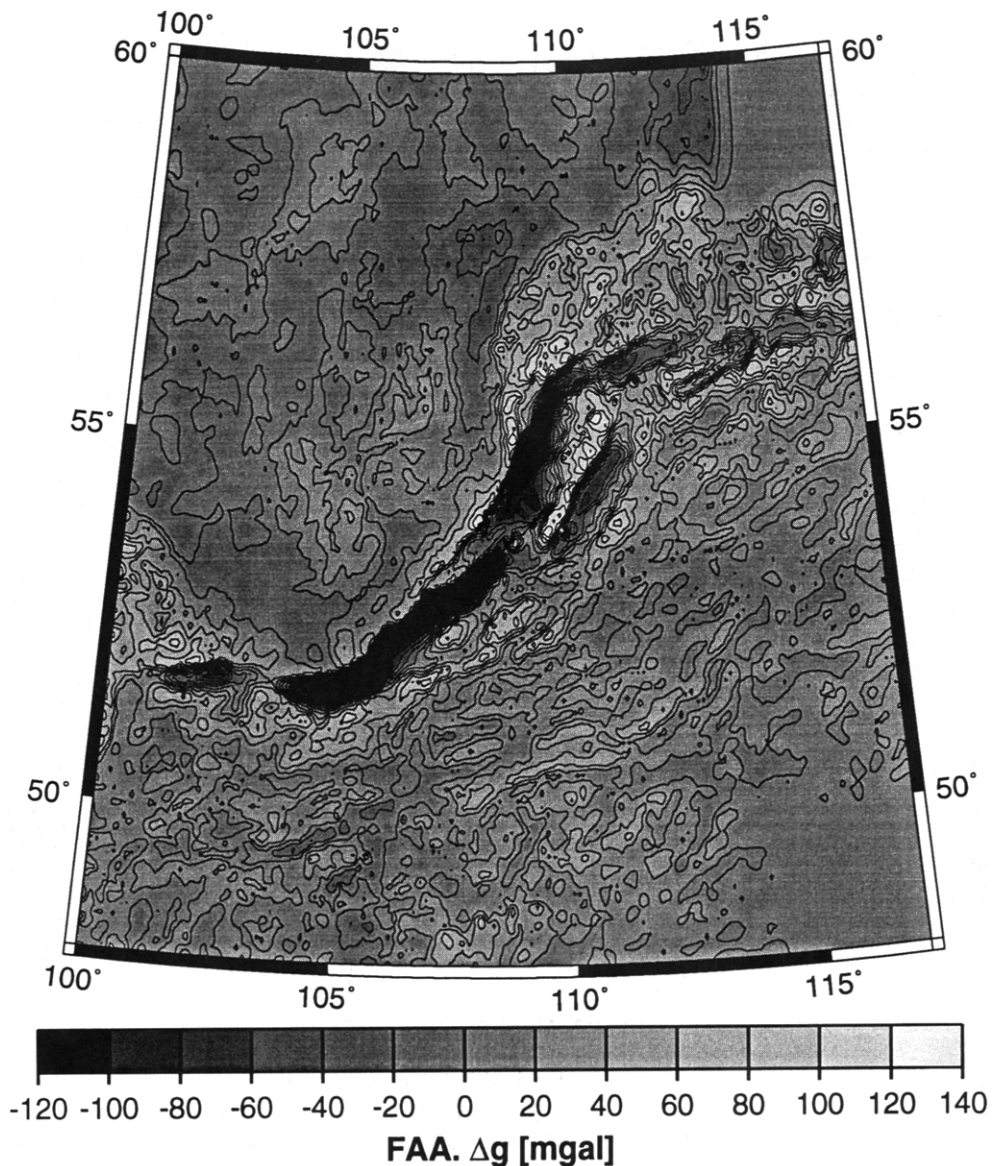

Fig. 1. Map of the free-air gravity anomaly over the Baikal Rift Zone.

previously obtained in the Upper Angara basin [23], located in the NBR (Fig. 2).

We have computed a simple Bouguer Anomaly (BA) for each profile, using an average, commonly used density value of 2670 kg/m^3 for topography loads and for the whole crust [33,29,23]. These

previous studies have shown that terrain corrections are very small over the BRZ. We therefore do not take them into account for the present study. The effect of density variations due to water and sediment infills inside the rift basins was corrected using bathymetric cross-sections and geophysical data on
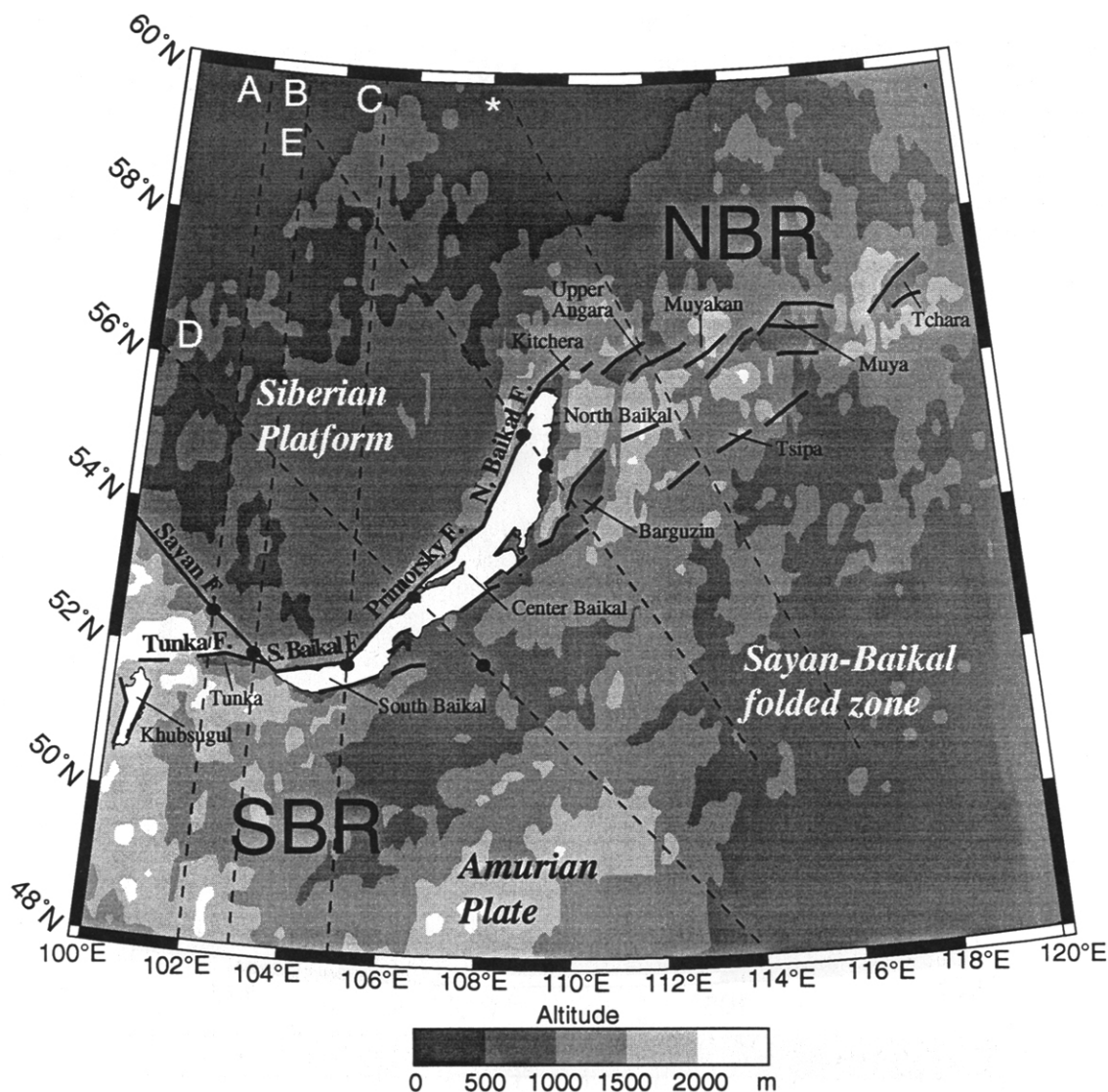

Fig. 2. Structural map of BRZ with average topography (grey shades). Thick lines are major rift faults; dashed lines are modelled profiles (this study), indicated by a letter. Asterisk indicates the profile modelled by [23]. Dots are plate discontinuities used for plate flexure modelling. Fault names cited in the text are indicated (in bold), as well as main rift depressions. *SBR* = South Baikal Rift, *NBR* = North Baikal Rift.

basement structure [26,32]. The density assumed for rift sediment infill is 2250 kg/m³ [33]. This simple correction allows us to remove most of the short-wavelength negative BA peak observed over the basins, except for profile C (Fig. 3). The density contrast associated with the Moho discontinuity is 630 kg/m³ [23].

In order to explain the observed BA, we first test several traditional continuous plate models involving a regional (flexural) compensation of the surface topography (acting as a vertical, horizontally distributed load) and boundary loads (e.g., produced by the interaction between lithospheric plates). As usual, we begin from simple flexural models based on elastic plate approximation. Then we explore more realistic models based on a brittle–elasto-ductile, quartz-dominated crust/olivine-dominated mantle

rheology [34]. These models involve power law stresses and exponential temperature dependence of the deformation rates ($\dot{\varepsilon}$ within the lithosphere (i.e. [35,36]):

$$\dot{\varepsilon} = A^* \exp(-H^*/RT)(\sigma_1 - \sigma_3)^n \qquad (1)$$

Where A^* is a material constant ($A^* = 5.6 \times 10^6$ MPa^{-n} sec^{-1} and 4.8×10^6 MPa^{-n} sec^{-1} for quartz and olivine, respectively; H^* is the activation enthalpy ($H^* = 0.19 \times 10^6$ J mol^{-1} and 0.533×10^6 J mol^{-1} for quartz and olivine, respectively); $R = 8.3144$ J (mol·K)$^{-1}$ is the gas constant; T is the absolute temperature at the given depth; and n is the power law exponent ($n = 3$ and 3.5 for quartz and olivine, respectively). The condition of brittle failure
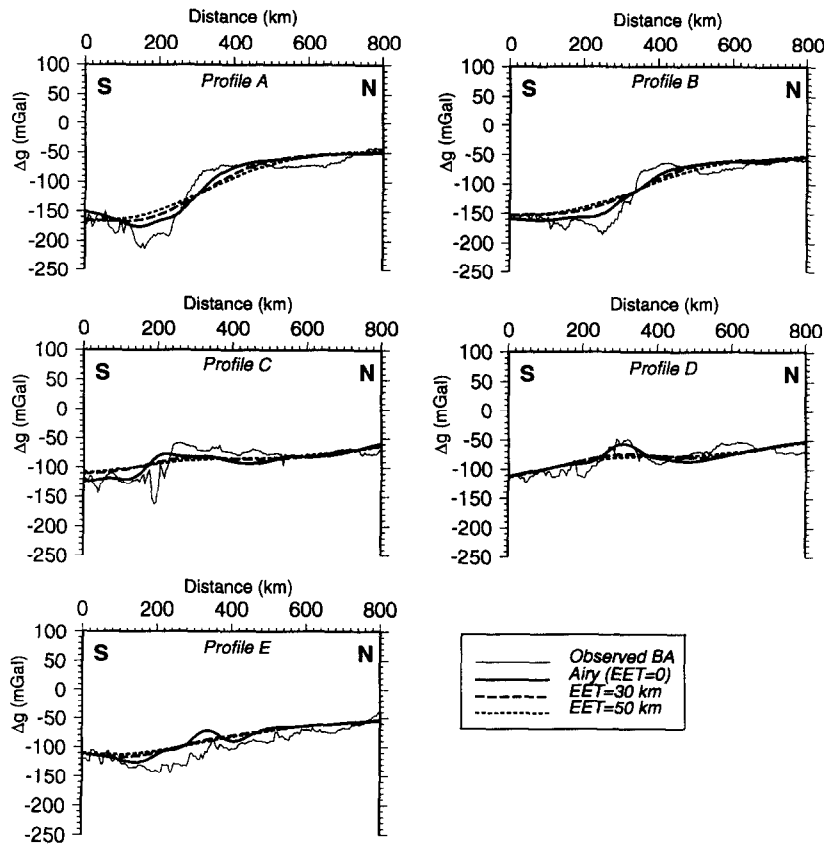

Fig. 3. Continuous elastic plate models using different EET values of 0, 30 and 50 km (thick lines), compared to observed BA (thin line). See comments in the text and corresponding RMS values in Table 1.

in the uppermost crust and mantle is analogous to the Von Mises criterion [37]:

$$\sigma_2 = (\sigma_1 - \sigma_3)/3.9 \text{ for } \sigma_3 < 120 \text{ MPa} \qquad (2)$$

$$\sigma_2 = (\sigma_1 - \sigma_3)/2.1 - 100 \text{ for } \sigma_3 \geq 120 \text{ MPa} \qquad (3)$$

where σ_1, σ_2 and σ_3 are the principal stresses.

The mechanical models based on brittle–elasto-ductile rheology laws allow us to account for a realistic stress distribution in the lithosphere, and for the distribution of inelastic brittle and ductile behaviours. Thus, they account for the ability of the lithosphere to localize deformations caused by external loads.

The average effective elastic thickness is relatively high in the BRZ (about 50 km, see [29]) compared to other continental rift zones, but it is much lower than the maximum mechanical thickness that could be expected for a lithosphere of this thermal age (400–700 Ma, see [26]) assuming a strong lower crust and, consequently, no mechanical crust/mantle decoupling [34]. EET values of about 50 km observed throughout the region would suggest that the lithospheric strength is reduced on a large scale due to a mechanical crust/mantle decoupling [34]. This phenomenon can occur in the presence of a weak lower crust with a low temperature of creep activation [38]. Therefore, we choose a low temperature creep activation rheology (i.e., quartz-dominated) for the whole crust. It is worth noting that the possible presence of an intracrustal low velocity zone in the Baikal rift [39] might be associated with this weak crustal rheology.

To model the mechanical response of the lithosphere, we use the same approach as in the numerical scheme presented in [23]. It is based on the solution of mass, momentum and energy conservation equations, in an assumption of a thin brittle-elasto-ductile plate. We solve the problem of lithospheric deformation assuming starting temperature distribution and yield-stress profiles derived from the solution of the heat transfer problem in the continental lithosphere [38], for a thermal age of about 400 Ma [26], and a low strain rate of about $1 \div 3 \times 10^{-15}$ sec^{-1}, estimated from field observations [40] and first GPS measurements [41].

Complex rheology profiles can be simply described by three parameters [42]: the maximum

Table 1
Plate parameters used for plate flexure modelling

Profile	T_c (km)	h_1 (km)	h_2 (km)
A	CT = 45	CT = 15	CT = 85
B	CT = 44	CT = 14	CT = 85
C	CT = 42	CT = 20	CT = 95
D	var: 42–50	var: 14–20	var: 85–95
E	CT = 42	CT = 20	CT = 95

CT = constant plate parameters. var = variable plate parameters (extreme values). See text for T_c, h_1 and h_2.

thickness of the competent crust (h_1), the total crustal thickness (T_c), and the depth of the bottom of the mechanical lithosphere (h_2). The value of h_1 is controlled by surface heat flow and is limited to 15–20 km for the BRZ. Previous seismic and gravity studies give an estimation of average T_c values used for initial reference models. It is possible to constrain h_2 from average EET estimates [34]:

$$h_2 \approx \left(\text{EET}^3 - h_1^3\right)^{1/3} + T_c$$

These initial parameters are listed in Table 1.

2.2. Modelling results

2.2.1. Continuous elastic plate models

We use for elastic plate models EET values of 0 (Airy compensation), 30 and 50 km, without horizontal extension (Table 2 and Fig. 3). Generally, at far distances from the rift axis, local or regional isostasy models seem consistent, because the relatively flat topography observed at the extremities of the profiles does not allow one to distinguish between local or regional compensation [23]. Near the rift axis the amplitude and the wavelength of the

Table 2
RMS variations associated with elastic plate models

	EET = 0	EET = 30 km	EET = 50 km
Profile A	17.232	23.177	27.478
Profile B	17.862	22.616	25.096
Profile C	21.809	21.559	22.582
Profile D	13.857	14.989	14.449
Profile E	22.502	21.776	22.000

Columns 2–4 show RMS (in mGal) variations depending on the effective elastic thickness (EET).

observed BA is always poorly reproduced by continuous plate models, especially for high EET values (Fig. 3). Note that, on profiles D and E (Fig. 3), the observed BA on both rift sides is lower than predicted by local isostasy models. This is visible on profile D on both parts of the axial relative high (km 100–250 and km 360–440); profile E shows a generalized low BA which extends from km 100 to 700.

Given the hypothesis that the observed BA, at wavelengths of about 100–1000 km, is mainly linked to the Moho geometry, we infer that surface loading (topography) applied on an elastic plate of variable effective thickness is not able to reproduce the observed Moho geometry. Current external sources of stress, as well as plate heterogeneities, must be taken into account.

2.2.2. Parameters of discontinuous continental plate models

We thus introduce in the models at least one plate discontinuity separating two flexured domains. Its initial location is constrained by geological and geophysical observations. For example, present-day tectonics and kinematics deduced from field studies, stress tensor analysis and GPS measurements indicate that the deformation in the southern part of the rift is accommodated by reverse-sinistral and normal-sinistral motions along the Sayan and south Baikal faults, respectively [43,30,44]. These faults, located on the Paleozoic suture between the Siberian craton and the Sayan–Baikal belt (Fig. 2), seem to behave as major lithospheric weaknesses accommo-

dating the current rift deformation. In the central and northern parts of the rift, previous analyses also showed that the Primorsky, north Baikal and Barguzin faults (Fig. 2) are three major active structures acting as normal faults [32,45]. The position of these discontinuities is then slightly adjusted in order to provide the best fit to the gravity data.

Mechanical plate discontinuities are modeled by near vertical free-slip bands. A detailed study comparing several models with variable elastic thicknesses, necking levels and fault geometries for the central Baikal basin area is presented elsewhere [28]. Unlike the latter study, we do not attempt here to constrain a possible fault geometry, detachment or necking depth but, instead, to represent a zone of lithospheric weakness able to localize the current deformation. To account for a more realistic rheology, we use a brittle–elasto-ductile plate model based on continental rheological profiles of the BRZ, as described above (Table 1). An important advantage of this procedure is that the use of plate discontinuities coupled with a realistic rheology allows quantitative estimation of the actual stresses acting at plate boundaries. Indeed, the elastic rheology does not seem a convenient approximation for the long-term properties of the rocks, since it often leads to self-inconsistent stress predictions [34].

We test both upward and downward bending of the plates by the use of vertical forces, as well as compressional and extensional horizontal forces. Different values of effective vertical and horizontal forces are tested, within $0-5e^{12}$ N/m. In the pre-

Table 3

RMS variations due to vertical forces applied on continental plates

S/N plates (N/m)	Profile A	Profile B	Profile C	SE/NW plates (N/m)	Profile D	Profile E
$0e^{12}/0e^{12}$	18.856	16.693	20.071	$0e^{12}/0e^{12}$	13.493	17.470
$0.5e^{12}/-0.5e^{12}$	16.486	13.744	17.613	$0.5e^{12}/0.5e^{12}$	9.477	11.540
$1e^{12}/-1e^{12}$	14.746	11.469	15.983	$1e^{12}/1e^{12}$	9.305	8.563
$1.5e^{12}/-1.5e^{12}$	13.835	10.259	15.459	$1.5e^{12}/1.5e^{12}$	13.140	11.241
$2e^{12}/-2e^{12}$	13.841	10.415	16.138	$2e^{12}/2e^{12}$	18.675	17.131
$2.5e^{12}/-2.5e^{12}$	14.697	11.812	17.866	$2.5e^{12}/2.5e^{12}$	24.809	23.994
$3e^{12}/-3e^{12}$	16.204	14.012	20.367	$3e^{12}/3e^{12}$	31.204	32.246

Columns 1 and 5 describe the effective vertical force (in N/m) applied on both sides of the modelled plate discontinuity; that is, on the southern and northern plates, for the N–S trending profiles (A, B and C) and on the southeastern and northwestern plates for the SE–NW trending profiles (D and E). Positive and negative values depict downward and upward acting forces, respectively. Columns 2–4, 6 and 7 show the RMS (in mGal) variations for the corresponding profiles. No horizontal force is applied in this model.

sented models the average stress values are of the order of 200-300 MPa, which is in agreement with geodynamic considerations and yield-stress rheology based on experimental rock mechanics results [37]. Vertical forces are necessary to model plate interaction and out-of-plane components of the stresses acting on the rift sides (horizontal included) and the effects of unknown heterogeneities. As already reported by [46], relatively weak vertical forces have more important effects on the lithospheric flexure than much stronger horizontal forces. In turn, horizontal forces have more important effects on the volumetric deformation and weakening of the lithosphere.

Plate flexure results in a Moho geometry, which is used to compute the theoretical (modeled) BA and to assess the crustal structure. Relative T_c estimates between different points of a given profile are constrained within less than 1 km uncertainty by plate flexure computation. Conversely, it is worth noting that absolute T_c values depend on the initial reference models used; hence they may be linked to greater uncertainties (about 3-4 km).

3. Results of modelling

The models were refined by modifying forces and plate parameters until the RMS (Root Mean Square) residual could not be significantly reduced. Tables 3 and 4 present some of the various models tested and their associated RMS. The profiles located in the SBR (A, B and C) depict a strong N-S asymmetry, which decreases in amplitude from west to east (Fig. 4). The use of the Sayan and south Baikal fault as plate discontinuities is convenient and allows us to constrain a well fitting plate flexure (Fig. 2). These modeled profiles are characterized by an upward flexure of the northern plate and a downward flexure of the southern plate, resulting in a positive Moho step in the north of about 15, 10 and 5 km for profiles A, B and C, respectively (Table 3 and Fig. 4). The thickness of the Siberian craton (northern plate) does not vary significantly between those profiles (around 45 km); conversely, the Amurian (southern plate) crust thickness changes from 50-60 km in the west (profile A) to 43-48 km in the east (profile C). The overthickened crust of the Sayan-

Table 4
RMS variations due to horizontal forces applied on continental plates

Horizontal force	Profile A	Profile B	Profile C	Profile D	Profile E
$-2.5e^{12}$	15.559	10.883	14.243	8.354	7.526
$-2e^{12}$	15.244	10.671	14.131	8.502	7.584
$-1.5e^{12}$	14.897	10.488	14.390	8.612	7.678
$-1e^{12}$	14.524	10.356	14.607	8.785	7.827
$-0.5e^{12}$	14.176	10.281	14.948	9.044	8.093
$0e^{12}$	13.841	10.259	15.459	9.305	8.563
$0.5e^{12}$	13.634	10.221	16.185	9.604	9.099
$1e^{12}$	13.470	10.435	16.187	9.421	9.055
$1.5e^{12}$	12.855	10.516	16.278	8.979	9.225
$2e^{12}$	12.989	10.497	16.114	8.850	9.304
$2.5e^{12}$	13.758	10.937	15.995	8.905	9.321

Column 1 shows the effective horizontal force (in N/m) applied on the model. Positive and negative values depict compressional and extensional forces, respectively. Columns 2-6 show the RMS (in mGal) variations for the corresponding profiles. Vertical forces applied on each model are those associated with RMS minima, as seen in Table 3.

Tunka region has been previously observed by Russian teams, who reported a N-S change in the crustal thickness from 45 to 53 km across the Tunka fault (see [39], and fault location in Fig. 2), which is comparable to our results, taking into account their uncertainty.

Although RMS variations associated with the horizontal forces tested must be interpreted with care, it is worth noting that horizontal compressional forces improve the fit to models A and B, while extensional forces are required in model C (Table 4). This observation coincides fairly well with the results of stress tensor determination previously obtained by the use of earthquake focal mechanisms, which show a sharp change in tectonic regime from west to east, varying from compression to extension [30]. The location of our profiles allows us to confirm that the westernmost expression of divergence (i.e., rifting sensu stricto) occurs somewhere between 103°E and 105°E. Note that extension (profile C) does not seem to be accompanied here by any significant crustal thinning.

Profiles D and E involve two plate discontinuities delimiting a detached block beneath the rift axis (Fig. 4). In both cases its northern limit corresponds to the fault bounding the western shore of Lake Baikal: namely, the Primorsky and north Baikal faults

for profiles D and E, respectively (Fig. 2), which are known to be the major active faults of this area [43,28]. However, the southern block boundary does not seem to correlate with any major active fault. We propose that this second discontinuity may not represent an actual lithospheric fault but rather delimits the eastern boundary of a wide axial fractured zone

(i.e., the detached prism) located between two continuous plate domains. The deformation is more widespread in the central rift area, probably because this region has undergone more important stretching. Thus, unlike in the SBR region, the plate area where deformation localizes cannot be represented here by a single narrow discontinuity. Taking into account
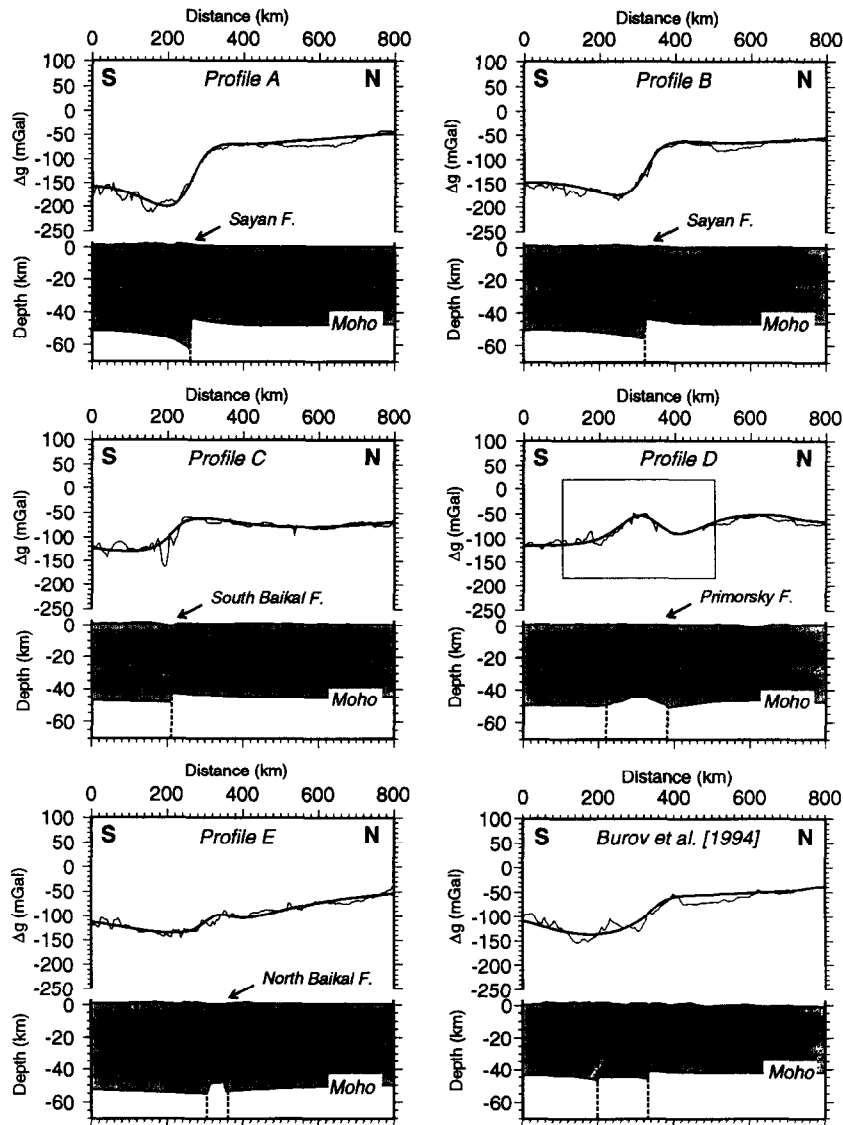
Fig. 4. Best-fit models (thick lines) using brittle–elasto-ductile rheology and plate discontinuities (vertical dashed lines). Thin line is the observed BA. Each profile is shown with the inferred crust thickness (grey area) and Moho geometry. Arrows represent the stresses applied at plate boundaries (horizontal arrows) or near plate discontinuities (vertical arrows). Note that vertical arrows do not necessarily represent the actual slip on active faults. Profiles A to E are presented in this study. The last profile (bottom-right corner) is after [23]. Inset on profile D corresponds to the area modelled by [28] along a similar profile.

their limited dimensions (50 and 160 km, respectively), we assume local compensation for the axial blocks. The resulting Moho surface is upwarped by about 7 km beneath the rift axis; corresponding crustal thinning is spread over a much wider area in the central (160 km) than in the northern rift (50 km). The plate flexure is directed downwards on both sides of the blocks, in order to model the relatively low BA observed besides the rift axis. The average plate thickness on both parts of the rift axis increases from 47–50 km in profile D to 49–53 km in profile E. Note the use of horizontal extensional forces improves the fit of these models, which is obviously in good agreement with the geodynamic context.

Unlike other profiles, the particular convex shape of the BA north of 400 km on profile D (Fig. 4) cannot be reproduced using constant rheological parameters and NW–SE plate flexure (Table 1). This misfit may, perhaps, not result from a local density anomaly, since this same intracratonic area is well fitted on profiles A, B and C. These profiles depict a strong N–S plate flexure and E–W variation in rheological parameters (Tables 1 and 3), which could be responsible for a 3D flexure of the Siberian plate. In order to model these variations and to simulate 3D plate flexure, we used variable plate parameters along profile D, as follows: plate parameters used for modelling profiles A, B, and C were attributed to profile D at the intersects with these 3 profiles, and linearly interpolated between them. This provides a good fit in the given area (Fig. 4), which means that N–S flexure, mainly related to compressional stresses (see profiles A and B) seems to have a strong effect on the mechanical behaviour of this part of the Siberian craton.

4. Discussion

4.1. Crustal and lithospheric structure

Our gravity models favour a high average crustal thickness over the whole rift zone (about 46–50 km for the Siberian plate, 44–47 km at the rift axis, and 50–55 km for the Sayan–Baikal folded zone). Crustal thinning mainly concerns the central part of the rift, where it reaches about 7 km and spreads over a 160 km wide area (Fig. 4). It is of comparable amplitude,

but of minor extent in the northern Baikal basin (50 km wide). This value of crustal thinning is quite consistent with the one deduced from geological observations [45]. In the SBR, the crust is clearly composed of two different parts: the southern ('Amurian') overthickened crust, and the northern ('Siberian') crust of constant thickness. Taking into account the uncertainties linked to absolute T_c estimates, these values seem still slightly higher than those described in previous studies, where the inferred crustal thickness is 34–40 km beneath the rift basins and 42–48 km beneath the surrounding ranges [47]. However, these authors assume a local isostatic compensation and a low density contrast at the Moho (240 kg/m^3), which consequently increase the amplitude of the modelled Moho topography.

In the central rift area the velocity structure inverted from teleseismic travel time residuals could advocate for an asymmetric upwarp of the lithosphere–asthenosphere transition [48], but the corresponding density contrast used by the authors (20 kg/m^3) appears much too low to be imaged by gravity modelling. Moreover, a near-surface asthenospheric upwelling should strongly modify the position of the rheological interfaces, which is not observed in our results: the bottom of the mechanical lithosphere (h_2) remains rather deep (85–95 km, see Table 1).

4.2. Plate flexure and rift-related topography

In order to complete this study, we compare our results to those previously obtained in the NBR using the same method [23]. Some similar features appear on profile E (north of Lake Baikal) and on the NBR profile: both depict an antisymmetric BA shape, with a 50 mGal step between the northern and southern extremities (Fig. 4). Both also depict a narrow positive BA peak at the rift axis, but its wavelength was too small to be considered in the previous modelling [23]. The main differences between these profiles are: (1) the width of the detached block (50 and 135 km for profile E and NBR profile, respectively); (2) the flexure of the northern plate, which is directed downward on profile E and upward on the NBR profile.

On profile D downward acting forces are needed to reproduce the observed BA; they result in crustal

roots on both sides of the rift axis. Two possible sources of additional positive (downward acting) loads (see, e.g., [3]) can be invoked: lower crustal thinning, implying the presence of dense mantle material at crustal levels, and basin sediment infill (about 3–4 km of rift sediments in the north Baikal basins, see [32]). These results contradict those presented by [28] in the central Baikal area, where an upward flexure of the plate is modeled in response to extensional tectonics. However, this latter modelling concerns a shorter part of the profile centred on the central Baikal basin (profile D), and may not allow one to describe the general sense of flexure (Fig. 4).

This central rift area is characterized by small reliefs bounding the rift depression (Fig. 2). Although they are much lower than those observed in the North Baikal and Sayan regions, their existence is difficult to explain in a context of downward plate flexure. Here the question is raised of rift-related and/or ante-rift reliefs, the latter possibly resulting from a tectonic phase of crustal thickening preceding the early stages of rifting. Recent analysis of microtectonic data and rift basins sediments seems to indicate that a 'proto-rift' phase, characterized by transpressional and compressional tectonics, took place somewhere between the final Cretaceous and the Miocene [32,31,49], and could have resulted in pre-rift mountain building in the BRZ.

Following the same hypothesis of downward plate flexure, the high (up to 3000 m) topography encountered in the NBR (profile E) should also be associated with deep crustal roots; that is, to a thickened crust, implying important ante-rift topography. However, this gravity modelling is based on the assumption of constant density contrast between the crust and the upper mantle. One must remember that a deep-seated negative density anomaly linked to anomalous, light upper mantle (see, e.g., [50]) could also be responsible for the long-wavelength low BA observed on profile E, and create buoyancy forces able to support the observed relief. This latter hypothesis must be taken into account and should be checked by other means, such as travel-time tomography, which should allow us to describe velocity variations within the crust and upper mantle.

Conversely, the mountains surrounding the Upper Angara and the south Baikal depressions are supported by an upward-flexured plate, possibly resulting from isostatic lithospheric rebound in response to extensional processes (e.g., [7]). Finally, in the westernmost part of the rift zone, the high relief observed south of the Sayan fault seems to be not due to rift tectonics sensu stricto but, apparently, results from the overthickening of the Amurian crust under compressional forces.

4.3. Tectonic forces

Horizontal extensional forces are modeled in the two profiles crossing Lake Baikal. West of the lake, horizontal extension abruptly gives place to increasing compressional forces, confirming the sharp change in tectonic regime already observed [30]. We can see here that the Paleozoic suture bounding the craton behaves as a major lithospheric weakness and acts as a rheological boundary between two plates of different character: in response to compression, the weak Amurian crust is thickening, while the resistant Siberian craton is undergoing a long-wavelength flexure (visible on profile D).

Comparing these results to stress tensors and fault motions deduced from earthquake focal mechanisms [30], we can propose that the thickening and downward bending of the Amurian plate west of Lake Baikal (profile A) is due to the propagation of SW–NE compression coming from the India–Asia collision (Fig. 5). This deformation seems to encounter a strong resistance when reaching the rigid Siberian craton, which impedes its northeastwards propagation. Here, again, we emphasize the role of the southwards pointing edge of the Siberian craton, acting as a passive indentor in response to convergence motions. This effect decreases eastwards (profile B) because the southern plate is able to escape to the east, causing reverse strike-slip faulting along the Sayan fault and oblique opening (profile C) along the south Baikal fault [30] (Fig. 5), which could explain the negligible amount of crustal thinning observed here. Further northwards (profile D), this motion is accommodated by 'typical' normal opening of the central Baikal basin along the eastern border of the craton. When approaching the NBR (profile E), crustal thinning seems much lower, possibly because the deformation is more diffuse. Let us recall that this part of the rift is developing inside the Sayan–Baikal folded zone (Figs. 2 and 5) and seems
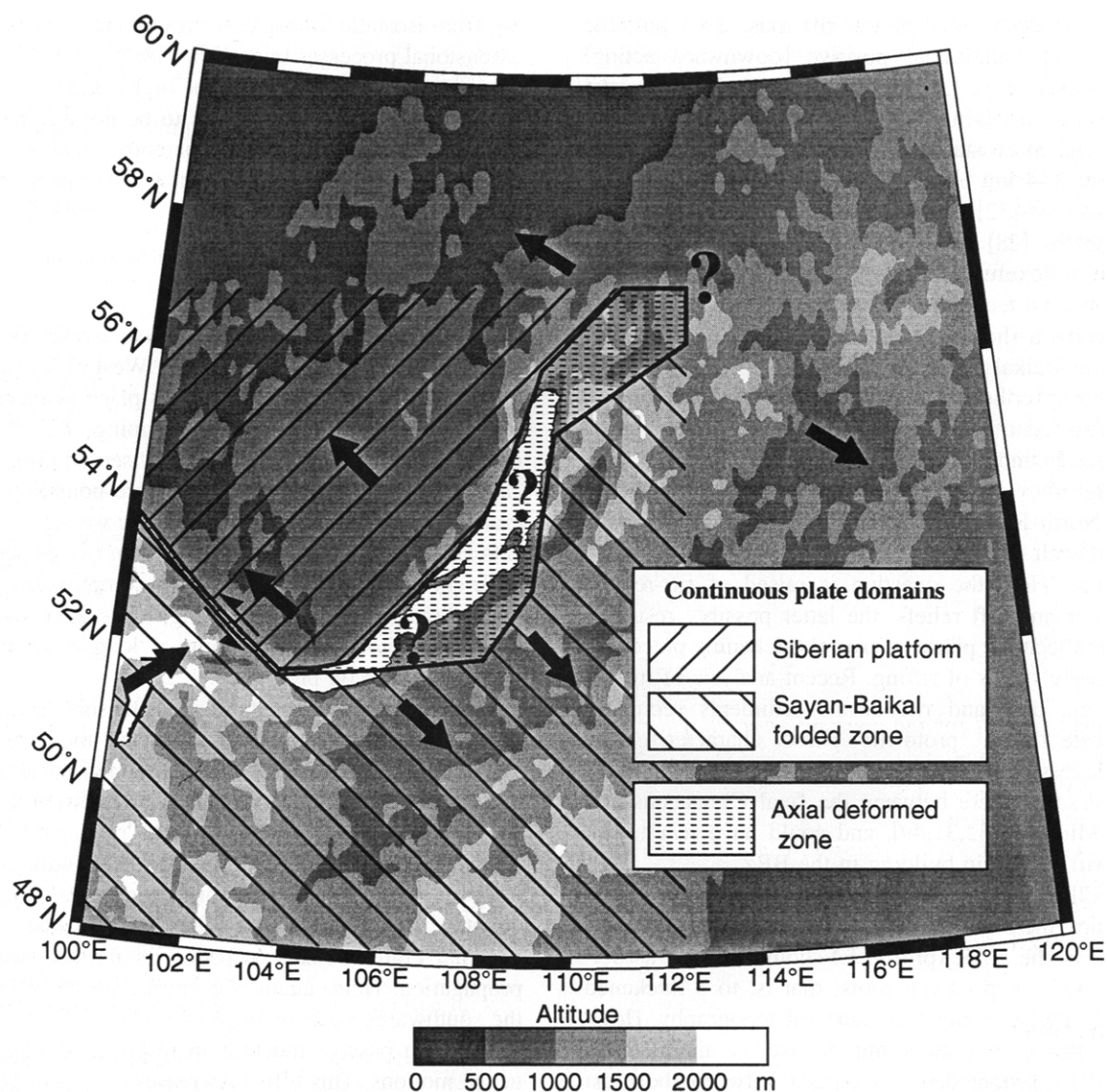
Fig. 5. Tectonic interpretation of the lithospheric deformation. Black arrows are average motion directions after [30] for the South Baikal Rift and after [45] for the North Baikal Rift. The continental plate domains and the axial deformed zone are indicated. Question marks indicate uncertain correlation between the modelled profiles.

characterized by a fan-like opening accommodated by crustal block rotations inside the deformed rift zone (see [23,30,45]).

5. Concluding remarks

The results presented here favour the role of horizontal, far-field motions in the opening of the

Baikal depression, combined with the effect of inherited structures, in agreement with the results of fault motion predictions issued from the analysis of earthquake focal mechanisms [30] and with the geological observations on active fault geometry and kinematics [45]. Numerical finite-element kinematic modelling [44] has been used to understand more clearly the interaction between the modeled strain field and the geometry of the Siberian plate, and to determine

whether this factor dominates or not over possible deep mantle effects. We show here that the upwarping of mantle material beneath the central and northern lake basins, associated with axial crustal thinning, seems very localized. The inferred value of crustal thinning (7 km) is fairly consistent with that deduced from geological neotectonic analysis (10 km) [40]. Moreover, this mantle upwarp does not seem to be linked to a major asthenospheric upwelling, since the observed bottom of the mechanical lithosphere is still deep. However, this study does not aim at precisely imaging the lithosphere–asthenosphere transition, nor at constraining the real origin of the observed mantle upwarp, which should be done by a general tomography of earthquake travel times and by a detailed analysis of the late Cenozoic to Quaternary volcanic rocks outcropping in several parts of the BRZ.

Acknowledgements

References

[1] M.H.P. Bott, Modelling the loading stresses associated with active continental rift systems, Tectonophysics 215 (1992) 99–115.

[2] D.P. Mc Kenzie, Some remarks on the development of sedimentary basins, Earth Planet. Sci. Lett. 40 (1978) 25–32.

[3] S.S. Egan, The flexural isostatic response of the lithosphere to extensional tectonics, Tectonophysics 202 (1992) 291–308.

[4] A.B. Watts, M. Torne, Crustal structure and the mechanical properties of extended continental lithosphere in the Valencia through (western Mediterranean), J. Geol. Soc. London 149 (1992) 813–827.

[5] J. Chéry, F. Lucazeau, M. Daignières, J.P. Vilotte, Large uplift of rift flanks: A genetic link with lithospheric rigidity?, Earth Planet. Sci. Lett. 112 (1992) 195–211.

[6] N.J. Kusznir, R.G. Park, The extensional strength of the continental lithosphere: Its dependence on geothermal gradi-

[7] K.J. Weissel, G.D. Karner, Flexural uplift of rift flanks due to mechanical unloading of the lithosphere under extension, J. Geophys. Res. 94 (1989) 13919–13950.

[8] P. Allemand, J.-P. Brun, Width of continental rifts and rheological layering of the lithosphere, Tectonophysics 188 (1991) 63–69.

[9] E.C. Parker, P.M. Davis, J.R. Evans, H.M. Iyer, K.H. Olsen, Upwarp of anomalous asthenosphere beneath the Rio Grande rift, Nature 312 (1984) 354–356.

[10] K.H. Olsen, W.S. Baldridge, J.F. Kallender, Rio Grande rift: An overview, Tectonophysics 143 (1987) 119–139.

[11] A.A. Nyblade, H.N. Pollack, D.L. Jones, F. Podmore, M. Mushayandebvu, Terrestrial heat flow in east and southern Africa, J. Geophys. Res. 95 (1990) 17371–17384.

[12] W.V. Green, U. Achauer, R.P. Meyer, A three dimensional image of the crust and upper mantle beneath the Kenya rift, Nature 354 (1991) 199–203.

[13] U. Achauer, P.K.H. Maguire, J. Mechie, W.V. Green, the K.W. Group, Some remarks on the structure and geodynamics of the Kenya rift, Tectonophysics 213 (1992) 257–268.

[14] K.-P. Bonjer, C. Gelbke, B. Gilg, D. Rouland, D. Mayer-Rosa, B. Massinon, Seismicity and dynamics of the upper Rhine graben, J. Geophys. 55 (1984) 1–12.

[15] P. Morgan, W.R. Seager, M.P. Golombek, Cenozoic thermal, mechanical and tectonic evolution of the Rio Grande rift, J. Geophys. Res. 91 (1986) 6263–6276.

[16] J.M. Larroque, A. Etchecopar, H. Philip, Evidence for permutation of stresses s1 and s2 in the Alpine foreland: The example of the Rhine Graben, Tectonophysics 144 (1987) 315–322.

[17] P.W. Lipman, N.A. Logatchev, Z.Y.A., C.E. Chapin, V. Kovalenko, P. Morgan, Intracontinental rift comparisons (Baikal and Rio Grande rift systems), EOS 9 (1989) 4.

[18] G.R. Keller, M.A. Khan, P. Morgan, R.F. Wendlandt, W.S. Baldridge, K.H. Olsen, C. Prodehl, L.W. Braile, A comparative study of the Rio Grande and Kenya rifts, Tectonophysics 197 (1991) 355–371.

[19] G.N. Shudofsky, S. Cloetingh, S. Stein, R. Wortel, Unusually deep earthquakes in East Africa: Constraints on the thermomechanical structure of a continental rift system, Geophys. Res. Lett. 14 (1987) 741–744.

[20] C.J. Ebinger, G.D. Karner, J.K. Weissel, Mechanical strength of extended continental lithosphere: constraints from the western rift system, East Africa, Tectonics 10 (1991) 1239–1256.

[21] S.V. Lysak, Heat flow variations in continental rifts, Tectonophysics 208 (1992) 309–323.

[22] J. Déverchère, F. Houdry, M. Diament, N.V. Solonenko, A.V. Solonenko, Evidence for a seismogenic upper mantle and lower crust in the Baikal rift, Geophys. Res. Lett. 18 (1991) 1099–1102.

[23] E.B. Burov, F. Houdry, M. Diament, J. Déverchère, A broken plate beneath the North Baikal rift zone revealed by gravity modelling, Geophys. Res. Lett. 21 (1994) 129–132.

[24] C. Petit, J. Déverchère, Velocity structure of the northern Baikal rift, Siberia, from local and regional earthquake travel times, Geophys. Res. Lett. 22 (1995) 1677–1680.

[25] N.N. Puzyrev, M.M. Mandelbaum, S.V. Krylov, B.P. Mishenkin, G.V. Petrik, G.V. Krupskaya, Deep structure of the Baikal and other rift zones from seismic data, Tectonophysics 45 (1978) 15–22.

[26] N.A. Logatchev, Y.A. Zorin, Baikal rift zone: Structure and geodynamics, Tectonophysics 208 (1992) 273–286.

[27] M. Diament, M.G. Kogan, Long wavelength gravity anomalies over the Baikal rift and geodynamic implications, Geophys. Res. Lett. 17 (1990) 1977–1980.

[28] P. van der Beek, Flank uplift and topography at the central Baikal Rift (SE Siberia): A test of kinematic models for continental extension, Tectonics (1997) in press.

[29] C. Ruppel, M.G. Kogan, M.K. McNutt, Implications of new gravity data for Baikal rift zone structure, Geophys. Res. Lett. 20 (1993) 1635–1638.

[30] C. Petit, J. Déverchère, F. Houdry, V.A. Sankov, V.I. Melnikova, D. Delvaux, Present-day stress field changes along the Baikal rift and tectonic implications, Tectonics 15 (1996) 1171–1191.

[31] N.A. Logatchev, History and geodynamics of the Lake Baikal Rift in the context of the Eastern Siberia rift system: A review, Bull. Centr. Rech. Explor.-Prod. Elf Aquitaine 17 (1993) 353–370.

[32] D.R. Hutchinson, A.J. Golmshtok, L.P. Zonenshain, T.C. Moore, C.A. Scholz, K.D. Klitgord, Depositional and tectonic framework of the rift basins of Lake Baikal from multichannel seismic data, Geology 20 (1992) 589–592.

[33] Y.A. Zorin, V.M. Koshevnikov, M.R. Novoselova, E.K. Turutanov, Thickness of the lithosphere beneath the Baikal rift zone and adjacent regions, Tectonophysics 168 (1989) 327–337.

[34] E.B. Burov, M. Diament, The effective elastic thickness (Te) of continental lithosphere: What does it really mean?, J. Geophys. Res. 100 (1995) 3905–3927.

[35] S.H. Kirby, A.K. Kronenberg, Rheology of the lithosphere: Selected topics, Rev. Geophys. 25 (1987) 1219–1244.

[36] D.L. Kohlstedt, B. Evans, S.J. Mackwell, Strength of the lithosphere: Constraints imposed by laboratory experiments, J. Geophys. Res. 100 (1995) 17587–17602.

[37] J.D. Byerlee, Friction of rocks, Pure Appl. Geophys. 116 (1978) 615–626.

[38] E.B. Burov, L.I. Lobkovsky, S. Cloetingh, A.M. Nikishin,

Continental lithosphere folding in Central Asia (part 2), Constraints from gravity and topography, Tectonophysics 226 (1993) 73–87.

[39] N.N. Puzyrev, Baikal interiors according to seismic data (in Russian), Izd. Akad. N. Sib. Otd., Novosibirsk, 1981.

[40] F. Houdry, Y. Gaudemer, V. Sankov, J. Déverchère, Geometry and rate of faulting during the Holocene in the North Baikal rift zone, Terra Nova 5, Abstr. Suppl. No 1 (1993) 259.

[41] O. Lesne, E. Calais, J. Déverchère, C. Petit, V. Sankov, K. Levi, Active deformation in the Baikal rift zone, Siberia, from GPS measurements, seismotectonic analysis and finite element modeling, EUG General Meet., March 23–27, Strasbourg, 1997.

[42] E.B. Burov, M. Diament, Isostasy, effective elastic thickness (EET) and inelastic rheology of continents and oceans, Geology 24 (1996) 419–422.

[43] S.I. Sherman, Faults and tectonic stresses of the Baikal rift zone, Tectonophysics 208 (1992) 297–307.

[44] O. Lesne, E. Calais, J. Déverchère, Finite element modeling of crustal deformation in the Baikal rift zone: new insights into the active–passive rifting debate, Tectonophysics, submitted.

[45] F. Houdry, Mécanismes de l'extension continentale dans le rift nord Baikal, Sibérie: Contraintes des données d'imagerie SPOT, de terrain, de sismologie et de gravimétrie, PhD Thesis, Univ. Pierre et Marie Curie, Paris VI, 1994, 350 pp.

[46] D.L. Turcotte, G. Schubert, Geodynamics: Application of Continuum Physics to Geological Problems, Wiley, New York, 1982, 450 pp.

[47] Y.A. Zorin, L. Cordell, Crustal extension in the Baikal rift zone, Tectonophysics 198 (1991) 117–121.

[48] S. Gao, P.M. Davis, H. Liu, P.D. Slack, Y.A. Zorin, N.A. Logatchev, M.G. Kogan, P.D. Burkholder, R.P. Meyer, Asymmetric upwarp of the asthenosphere beneath the Baikal rift zone, Siberia, J. Geophys. Res. 99 (1994) 15319–15330.

[49] D. Delvaux, R. Moeys, G. Stapel, C. Petit, K. Levi, A. Miroshnichenko, V. Ruzhich, V. Sankov, Paleostress reconstruction and geodynamics of the Baikal region, Central Asia. Part II: Cenozoic tectonic stress and fault kinematics, Tectonophysics, in press.

[50] S.V. Krylov, B.P. Mishenkin, Deep structure of the Baikal region from seismic data, Proc. 27th Int. Geol. Congr. Geophysics, Utrecht, V.S. Press, 1984, pp. 144–149.